

SANDIA REPORT

SAND2015-8534

Unlimited Release

Printed September 2015

Solid State Consolidation of Nanocrystalline Copper-Tungsten Using Cold Spray

Aaron C. Hall, Pylin Sarobol, Nicholas Argibay, Blythe Clark, Christopher Diantonio

Prepared by
Sandia National Laboratories
Albuquerque, New Mexico 87185 and Livermore, California 94550

Sandia National Laboratories is a multi-program laboratory managed and operated by Sandia Corporation, a wholly owned subsidiary of Lockheed Martin Corporation, for the U.S. Department of Energy's National Nuclear Security Administration under contract DE-AC04-94AL85000.

Approved for public release; further dissemination unlimited.



Sandia National Laboratories

Issued by Sandia National Laboratories, operated for the United States Department of Energy by Sandia Corporation.

NOTICE: This report was prepared as an account of work sponsored by an agency of the United States Government. Neither the United States Government, nor any agency thereof, nor any of their employees, nor any of their contractors, subcontractors, or their employees, make any warranty, express or implied, or assume any legal liability or responsibility for the accuracy, completeness, or usefulness of any information, apparatus, product, or process disclosed, or represent that its use would not infringe privately owned rights. Reference herein to any specific commercial product, process, or service by trade name, trademark, manufacturer, or otherwise, does not necessarily constitute or imply its endorsement, recommendation, or favoring by the United States Government, any agency thereof, or any of their contractors or subcontractors. The views and opinions expressed herein do not necessarily state or reflect those of the United States Government, any agency thereof, or any of their contractors.

Printed in the United States of America. This report has been reproduced directly from the best available copy.

Available to DOE and DOE contractors from

U.S. Department of Energy
Office of Scientific and Technical Information
P.O. Box 62
Oak Ridge, TN 37831

Telephone: (865) 576-8401
Facsimile: (865) 576-5728
E-Mail: reports@osti.gov
Online ordering: <http://www.osti.gov/scitech>

Available to the public from

U.S. Department of Commerce
National Technical Information Service
5301 Shawnee Rd
Alexandria, VA 22312

Telephone: (800) 553-6847
Facsimile: (703) 605-6900
E-Mail: orders@ntis.gov
Online order: <http://www.ntis.gov/search>



Solid State Consolidation of Thermodynamically Stable Nanocrystalline Metals Using Cold Spray

Aaron C. Hall*, Pylin Sarobol*, Nicholas Argibay[#], Blythe Clark[†], Christopher Diantonio[‡]

*Coatings and Additive Manufacturing

[#]Materials Mechanics & Tribology

[†]Radiation-Solid Interactions

[‡]FENG and Tube Lifecycle Engineering

Sandia National Laboratories

P.O. Box 5800

Albuquerque, New Mexico 87185-MS1130

Abstract

It is well known that nanostructured metals can exhibit significantly improved properties compared to metals with conventional grain size. Unfortunately, nanocrystalline metals typically are not thermodynamically stable and exhibit rapid grain growth at moderate temperatures. This severely limits their processing and use, making them impractical for most engineering applications. Recent work has shown that a number of thermodynamically stable nanocrystalline metal alloys exist. These alloys have been prepared as powders using severe plastic deformation (e.g. ball milling) processes. Consolidation of these powders without compromise of their nanocrystalline microstructure is a critical step to enabling their use as engineering materials. We demonstrate solid-state consolidation of ball milled copper-tantalum nanocrystalline metal powder using cold spray. Unfortunately, the nanocrystalline copper-tantalum powder that was consolidated did not contain the thermodynamically stable copper-tantalum nanostructure. Nevertheless, this does demonstrate a pathway to preparation of bulk thermodynamically stable nanocrystalline copper-tantalum. Furthermore, it demonstrates a pathway to additive manufacturing (3D printing) of nanocrystalline copper-tantalum. Additive manufacturing of thermodynamically stable nanocrystalline metals is attractive because it enables maximum flexibility and efficiency in the use of these unique materials.

ACKNOWLEDGMENTS

The authors would like to acknowledge David Beatty from the New Mexico Institute of Mining and Technology, Socorro, NM, USA for preparing the cold spray coatings and Tom Chavez (01816) for milling the CuTa powders.

Sandia National Laboratories is a multi-program laboratory managed and operated by Sandia Corporation, a wholly owned subsidiary of Lockheed Martin Corporation, for the U.S. Department of Energy's National Nuclear Security Administration under contract DE-AC04-94AL85000.

CONTENTS

Introduction.....	9
Materials and Methods	11
Results and Discussion	12
Analysis of Cryomilled Powder.....	12
Analysis of Cold Spray Deposits	14
Conclusions.....	20
References.....	21
Distribution	23

FIGURES

Figure 1 Bright field TEM images showing the dispersion of both Ta particles and.....	9
Figure 2 XRD showing Ta and Cu starting powders as well as two batches of CuTa cryomilled powders.	12
Figure 3 Higher magnification showing two CuTa peaks with apparent line broadening.	12
Figure 4 Bright field TEM image taken using the CM30 microscope showing a nanocrystalline microstructure in the first batch of cryomilled CuTa powder. A domain size of approximately 50 nm is visible in the powder. Unexpectedly, the powder contained a large number of voids. The TEM sample broke apart during FIB preparation making it difficult to analyze.....	13
Figure 5 Bright field TEM image taken using the CM30 microscope showing nanocrystalline microstructure in the second batch of cryomilled CuTa powder. The second batch of powder was much more cohesive than the first batch and exhibited minimal voiding. Lamellar domains approximately 50 nm in size are visible throughout the powder. Regions of Ta that didn't fully mix are also visible (dark ribbons top and bottom of image).	13
Figure 6 SEM image (top left) and four EDS maps showing the surface of the copper-tantalum deposit prepared using the first batch of cryomilled powder. The sample is primarily copper with discrete regions of tantalum. .	14
Figure 7 Bright field TEM image taken using the CM30 microscope, showing the microstructure of the cold spray CuTa deposit using the first powder batch. Importantly, the CuTa cold spray deposit contains over 2 microns of continuous film (primarily copper) clearly demonstrating particle consolidation. Nanocrystalline copper grains are visible throughout this consolidated area. A void and a ribbon of tantalum are visible at the bottom of the image.	15
Figure 8 Bright field TEM image taken using the CM30 microscope showing the cold sprayed CuTa deposit prepared using the first batch of cryomilled powder. A highly deformed, sub-100 nm grain structure is visible throughout the deposit.	15
Figure 9 HAADF image and EDS patterns taken using the AC-STEM. The copper rich nanocrystalline structure in the deposit prepared using the first batch of cryomilled powder is shown. EDS maps reveal no detectable tantalum dispersion in the copper grain or along the copper grain boundaries. This suggests insufficient mechanically alloy of the copper and tantalum powders.....	16
Figure 10 EDS spectrum from the region shown in Figure 9. The Tantalum peak, while real, is extremely small compared to the copper peak indicating that very little Ta is present in this region of the sample.....	16
Figure 11 Z-contrast image taken using the AC-STEM showing the cold spray deposit prepared using the second batch of cryomilled powder. The white regions in the image are Ta, the gray regions are Cu, and the dark gray regions are copper oxide. Heterogeneous mixing is visible, consistent with the powder analysis.	17

Figure 12. Bright field image taken using the CM30 microscope showing the CuTa deposit prepared using the second batch of CuTa powder. Regions of nanocrystalline copper are intermixed with large ribbons of tantalum.18

Figure 13 Upper left is HAADF image and EDS maps taken using the AC-STEM. This data from the cold spray deposit prepared using the second batch of cryomilled powder shows that copper, tantalum, and copper oxide are present as discrete regions in the deposit.18

Figure 14 Bright field image taken using the AC-STEM, showing the microstructure within a tantalum ribbon. The tantalum exhibits considerable FIB damage making the grain structure difficult to resolve. Nevertheless, tantalum grains ~ 100nm in size are visible in the lower right of this image, confirming the presence of a nanocrystalline microstructure in the tantalum ribbon.19

TABLES

Table 1 Microprobe data showing CuTa deposit composition. Data from associated with the first batch of cryomilled powder is shown on the top row. Data associated with the second batch of cryomilled powder is shown on the second row. The deposit made using the second batch of cryomilled powder contained considerably more oxide than the first batch. This impacted the desired 90at%Cu-10at%Ta ratio and may have contributed to lack of dispersion formation.19

NOMENCLATURE

AC-STEM	Aberration Corrected Scanning Transmission Electron Microscopy
at	atomic
Cu	Copper
EDS	Energy Dispersive X-ray Spectroscopy
FIB	Focused Ion Beam
g	gram(s)
He	Helium
in	inch(es)
mbar	millibar
min	minute(s)
mm	millimeters
m/s	meters per second
mm/s	millimeters per second
MPa	megapascals
N ₂	Nitrogen
nm	nanometer
SEM	Scanning Electron Microscopy
SLPM	Standard Liters per Minute
SNL	Sandia National Laboratories
STEM	Scanning Transmission Electron Microscopy
T	temperature
Ta	tantalum
wt	Weight
X	times
XRD	X-ray Diffraction
%	percent

INTRODUCTION

Nanostructured materials are of widespread interest to the scientific community because of the unique properties offered by these materials [1,2]. The high grain boundary content of nanocrystalline materials results in grain boundary properties contributing significantly to the bulk material properties. Dislocation behavior in nanocrystals is different from larger crystals and can result in significant strengthening of nanocrystalline metals [3,4]. One of the most challenging problems associated with nanocrystalline materials is the consolidation of these small powders into larger shapes that can be used for practical applications [2].

Here we describe an initial experiment to demonstrate solid state consolidation of a Copper-Tantalum nanocrystalline metal. Copper-Tantalum alloys are of specific interest because they have been shown to exhibit a thermodynamically stable nanocrystalline microstructure [4, 5,6]. Importantly, a dispersion of tantalum atomic clusters in copper is thought to be necessary for thermodynamic stabilization of copper-tantalum cryomilled alloys, Figure 1, [6]. Thermodynamic stabilization is thought to occur in such nanostructures due to multiple mechanisms related to solute drag created by the dispersion [6]. If a nanocrystalline copper-tantalum powder can be consolidated using cold spray this not only offers a route to preparation of bulk copper-tantalum, it also offers a route to additive manufacturing of nanocrystalline metals [7,8,9].

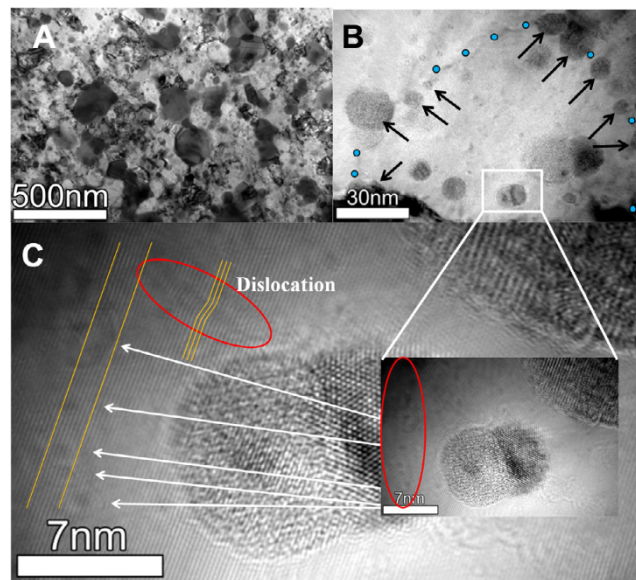


Figure 1 Bright field TEM images showing the dispersion of both Ta particles and atomic clusters at increasing magnifications, from [6]. A dispersion of Ta in copper is thought to be necessary to thermodynamic stabilization of copper-tantalum cryomilled alloys [6].

One approach to preparing bulk material with nanocrystalline microstructures is to use the cold spray process to consolidate a feedstock powder containing a nanocrystalline microstructure. Preparation of micron size powder containing a nanocrystalline microstructure by ball milling under liquid nitrogen (LN_2) is well known [5,2]. Ajdelsztajn has shown previously that cold spray can be used to successfully consolidate LN_2 ball milled powders containing a nanocrystalline microstructure (10-30 nm grain size) [11].

Cold spray is a well-known coating process in which a metal feedstock powder is sprayed at high velocity ($\sim 1000\text{m/s}$) and low temperature ($<100^\circ\text{C}$) [12]. A cold spray torch consists of a converging-diverging nozzle, a gas control system, a powder feed system, and a gas heater. Feedstock powder is injected into a high pressure ($> 200\text{psig}$) He or N_2 gas flow just upstream of a converging-diverging nozzle. The powder is entrained in the gas stream and reaches supersonic velocities as it travels through the nozzle. The propulsion gas stream is often heated to moderate temperatures ($< 600^\circ\text{C}$) in order to increase the sonic velocity of the gas and thus increase the particle velocity. Heating of the propulsion gas typically does not result in significant powder

heating [13]. Upon impact with the substrate the metal powder experiences significant mechanical deformation. This deformation forms an adiabatic shear instability at the particle-substrate contact which breaks surface oxides, induces shear at the particle-substrate interface, and ejects material from the particle-substrate interface [16,19,20,21,22]. Shear processes at particle/particle and particle/substrate interfaces result in solid-state metallurgical bonding [15,19,20,21,22]. High shear also results in significant plastic deformation of the impacting particle and the substrate surface [15,16,17,19,20,21,23]. As subsequent particles impact and consolidate a coating or bulk shape is formed [14,15,16]. Process vectors for cold spray are well understood. As particle velocity increases deposition efficiency, coating density, residual stress, and coating adhesion strength all increase [13].

Mechanical properties of both the substrate and the impacting particle significantly affect the total energy required for deposition and affect the deposit characteristics. Multiple computational studies show that critical velocity (velocity where there is sufficient kinetic energy for particle adhesion) is inversely dependent on particle density [19,24,25,26]. As density increases critical velocity is expected to decrease, all other properties remaining constant. Other studies show that deformation need not take place throughout the impacting particle for bonding to occur. Ultrafine grained regions have been observed in the particle boundaries of cold spray deposits suggesting that high shear is needed to enable bonding but that the entire particle need not shear [19,21,22,23,27].

The mechanisms responsible for nanocrystal formation during the ball milling process are also well understood. Fecht [11] explains that nanocrystals form during severe plastic deformation in three stages. Initially high density arrays of dislocations are formed. As plastic deformation continues these dislocations annihilate and recombine forming sub-grains with low angle grain boundaries. Further deformation causes the sub-grains to rotate forming high angle grain boundaries.

Work reported here clearly demonstrated that cold spray can be used to refine the microstructure of an ultra-fine-grained (100's of nm grain size) powder and consolidate it to create a homogenous nanocrystalline (20-40nm) microstructure [17]. When compared to the work of Ajdelsztajn which shows that the cold spray process can be used to consolidate nanocrystalline aluminum without causing recrystallization it illustrates the flexibility of the cold spray process. This flexibility is typical of spray processes and highlights the need to further understand the process-microstructure-property relationships in nanocrystalline cold spray coatings. The cold spray process is likely an extremely controllable method for preparing metal coatings and bulk metal shapes with homogenous nanocrystalline microstructures. If grain refinement in the cold spray process is occurring by the mechanism proposed by Fecht [5] cold spray should be capable of preparing nanocrystalline microstructures from almost any sprayable metal feedstock [18].

MATERIALS AND METHODS

All Copper Tantalum powders were made by liquid nitrogen ball milling (cryomilling) Metco 55 Copper and Amperit 150.074 Tantalum powders. Cryomilling was conducted with the intent of preparing a powder containing 90 atomic %Cu and 10 atomic %Ta based on [6]. All cryomilling was conducted using an Attrition mill model 01-HD made by Union Process (Akron, Ohio). Each powder was first weighed out in the appropriate ratios for copper 10 atomic % tantalum. The powders were then treated with liquid nitrogen prior to being placed into the attrition milling vessel. The attrition milling vessel, rotator shaft and arms/paddles and milling media were also pretreated with liquid nitrogen. The cold powders were then placed into the stainless steel attrition milling vessel and yttria stabilized zirconia (YSZ) milling media was added to a level just above the stainless steel rotator arms/paddles on the milling shaft. Liquid nitrogen was then added to the vessel. The powder was then attrition milled at 400RPM for a proscribed time. Liquid nitrogen was repeatedly introduced into the vessel to maintain a constant level during the milling process. This general process is repeated in subsequent steps, each time stepping down the size of the milling media. Milling was started using 5mm for the proscribed time. The milling media was then removed via sieving and the procedure was repeated using 2mm, then 1mm, and finally 0.5mm YSZ milling media. Two batches of CuTa powder were ball milled. Both batches followed identical milling procedures with the exception of the proscribed milling time for each step. In the case of the first powder batch milling was conducted 2 hours at each media size. In the case of the second powder batch, milling was conducted for 4 hours at each media size.

All cold spray was conducted using a system that was designed and built by Ktech Corporation (Albuquerque, NM). The cold spray nozzle had a 1.6mm diameter throat, a 100mm long supersonic region, and a 6.35mm diameter exit orifice. Helium was used as the accelerating gas. All samples were prepared using a raster speed of 50 mm/s and a standoff distance of 35 mm. The cryomilled Cu-Ta powder was sprayed using a 1.72 MPa, 350°C accelerating gas flow. In all cases, the powder feed gas pressure was 5% higher than the accelerating gas pressure. Cold spray coatings 0.127 mm thick were successfully obtained by spraying onto 6061 Al substrates.

Diffraction-contrast imaging was performed with a Philips CM30 TEM operated at 300 keV. Z-contrast imaging was performed with an FEI-Titan G80-200 AC-STEM microscope operated at 200 keV. Chemical composition analysis was performed by energy dispersive spectroscopy (EDS) spectrum imaging.

All microprobe analysis was conducted using a JEOL JXA-8530F, Field Emission Electron Probe MicroAnalyzer operated at 20keV, with a 20nA, 300µm beam diameter. Each analysis matrix was 11 x 9 points with a 2.97 x 2.11 mm area for a total of 99 points.

RESULTS AND DISCUSSION

Analysis of Cryomilled Powder

X-ray diffraction data was collected from both the raw copper and tantalum powders as well as each of two batches of cryomilled copper-tantalum powder. That data is shown in Figure 2 and Figure 3. The x-ray diffraction data confirm that the raw powders were copper and tantalum with no significant contaminants. Apparent peak broadening is visible in both batches of cryomilled powders, Figure 3, suggesting that the powders are at least partially nanocrystalline.

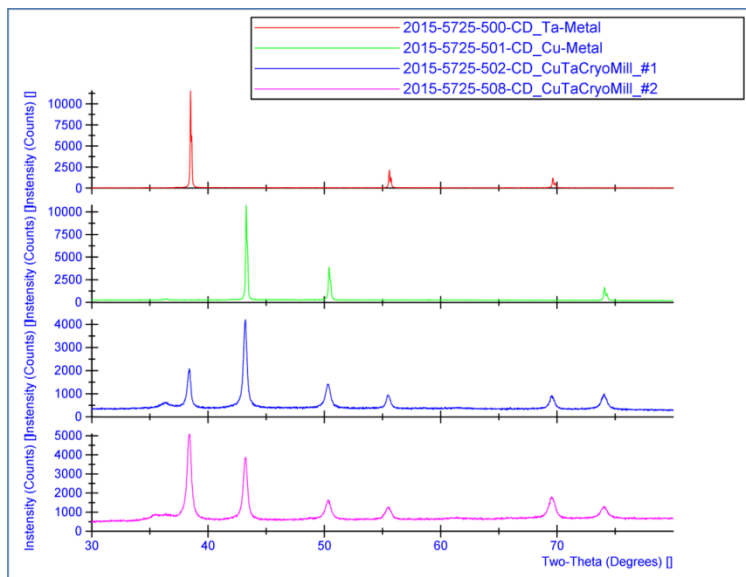


Figure 2 XRD showing Ta and Cu starting powders as well as two batches of CuTa cryomilled powders.

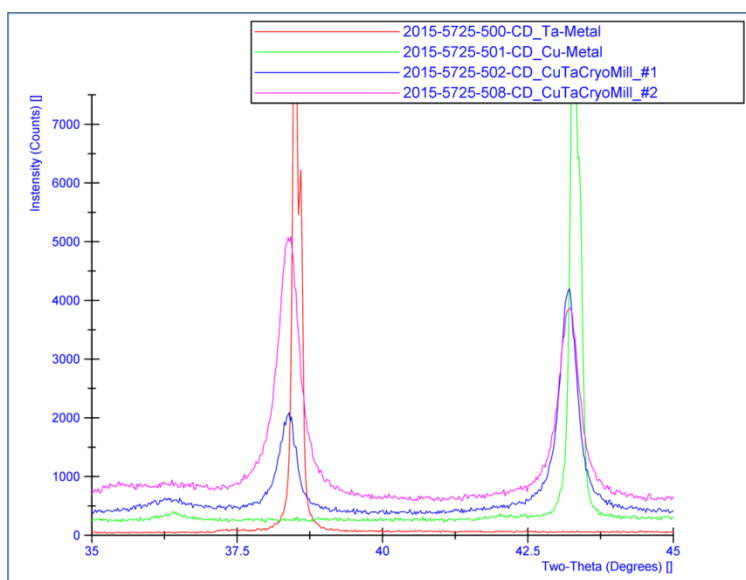


Figure 3 Higher magnification showing two CuTa peaks with apparent line broadening.

TEM images showing the powder microstructure in each batch of cryomilled copper-tantalum are shown in Figure 4 and Figure 5. In both cases the TEM images show nanocrystalline copper interlaced with bands of nanocrystalline tantalum. This demonstrates that the cryomilling process imparted sufficient plastic deformation to the raw powders to cause grain refinement and create a nanocrystalline microstructure. It also shows that the copper and tantalum have not fully mixed. Specifically, a dispersion of tantalum clusters in copper similar to that reported by [6] is not present in either sample. A dispersion of tantalum clusters in copper is thought to be necessary to thermodynamic stabilization of copper-tantalum [6].

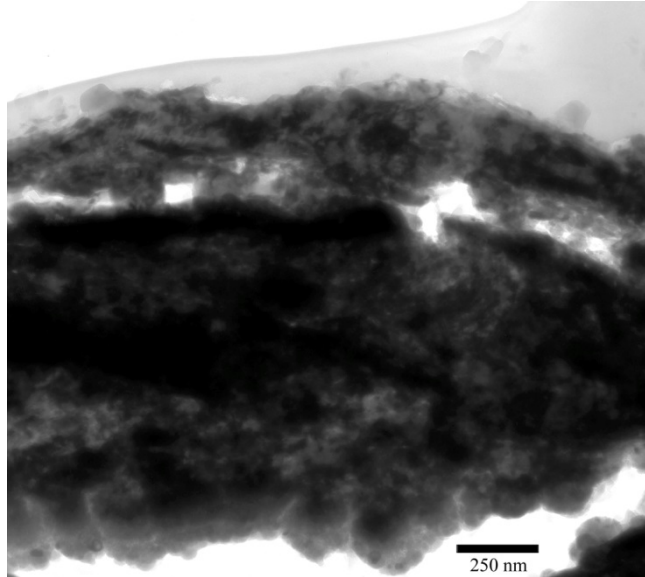


Figure 4 Bright field TEM image taken using the CM30 microscope showing a nanocrystalline microstructure in the first batch of cryomilled CuTa powder. A domain size of approximately 50 nm is visible in the powder. Unexpectedly, the powder contained a large number of voids. The TEM sample broke apart during FIB preparation making it difficult to analyze.

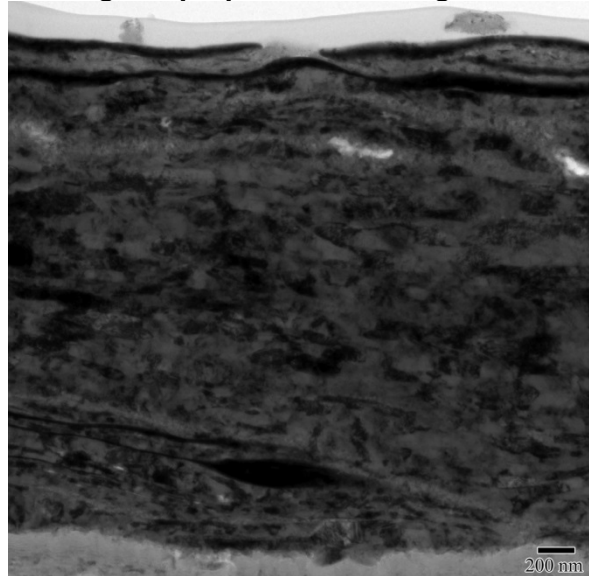


Figure 5 Bright field TEM image taken using the CM30 microscope showing nanocrystalline microstructure in the second batch of cryomilled CuTa powder. The second batch of powder was much more cohesive than the first batch and exhibited minimal voiding. Lamellar domains approximately 50 nm in size are visible throughout the powder. Regions of Ta that didn't fully mix are also visible (dark ribbons top and bottom of image).

Analysis of Cold Spray Deposits

Despite imperfect mechanical alloying, both cryomilled powders were cold sprayed and copper-tantalum deposits were successfully prepared in both cases. SEM analysis was used to confirm that the copper-tantalum powder deposited on the substrate. Figure 6 shows an SEM image and four EDS maps of the copper-tantalum deposit prepared using the first batch of cryomilled powder. The deposit is primarily copper but contains discrete regions of tantalum.

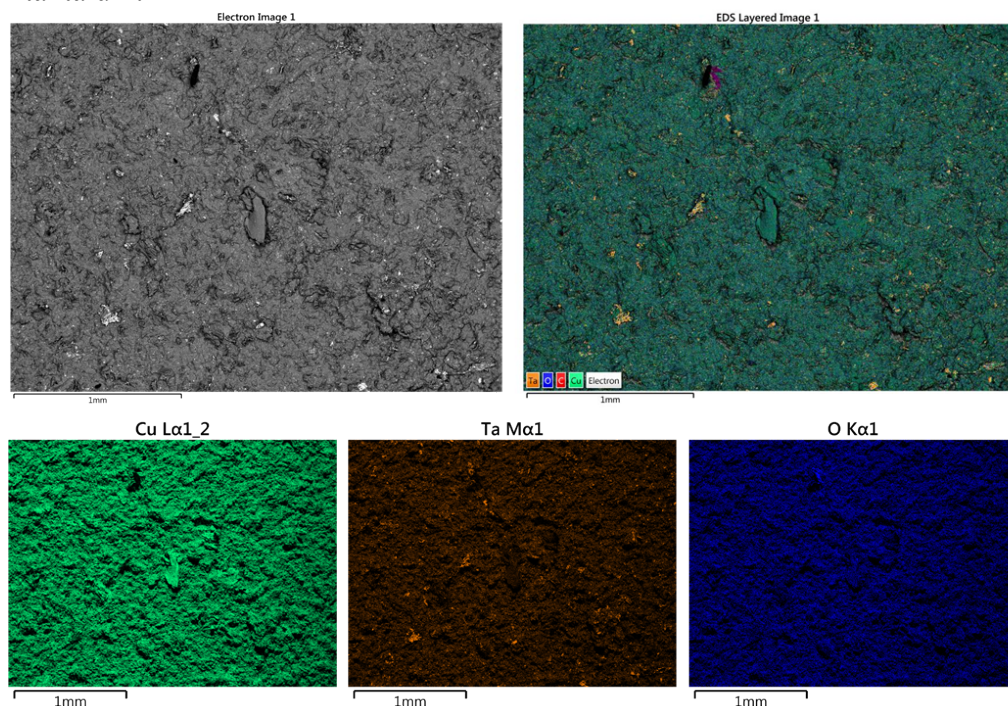


Figure 6 SEM image (top left) and four EDS maps showing the surface of the copper-tantalum deposit prepared using the first batch of cryomilled powder. The sample is primarily copper with discrete regions of tantalum.

TEM images showing the coating microstructures are shown below. Importantly, a nanocrystalline grain structure is visible throughout both coatings. This demonstrates that the cold spray process did not cause recrystallization or grain growth in the copper-tantalum cryomilled powder. However, like the powders, the coating microstructure is a mixture of discrete nanocrystalline copper and nanocrystalline tantalum regions not a nanocrystalline dispersion of tantalum atomic clusters in a copper matrix.

Figure 7 and Figure 8 show the cold spray deposit prepared using the first batch of cryomilled copper-tantalum powder.

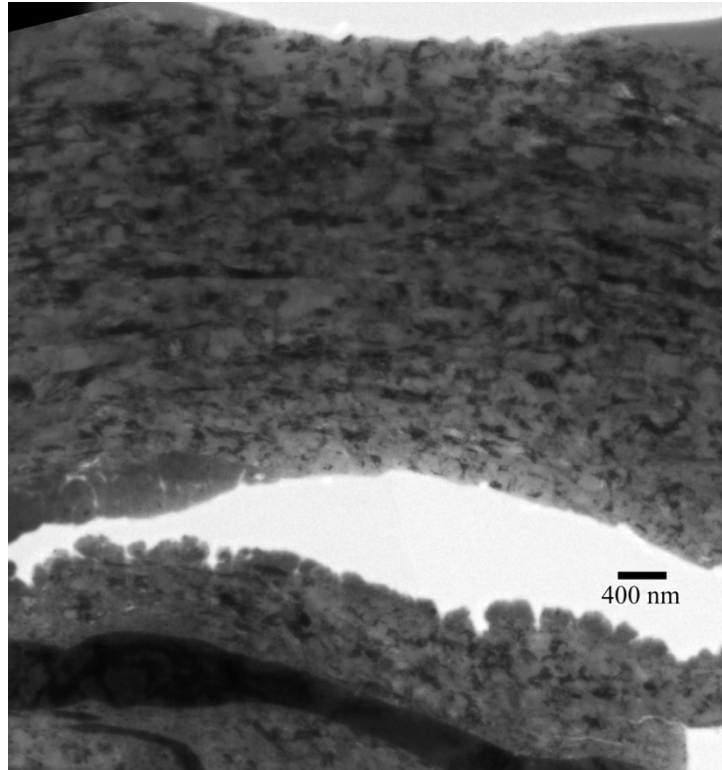


Figure 7 Bright field TEM image taken using the CM30 microscope, showing the microstructure of the cold spray CuTa deposit using the first powder batch. Importantly, the CuTa cold spray deposit contains over 2 microns of continuous film (primarily copper) clearly demonstrating particle consolidation. Nanocrystalline copper grains are visible throughout this consolidated area. A void and a dark ribbon of tantalum are visible at the bottom of the image.

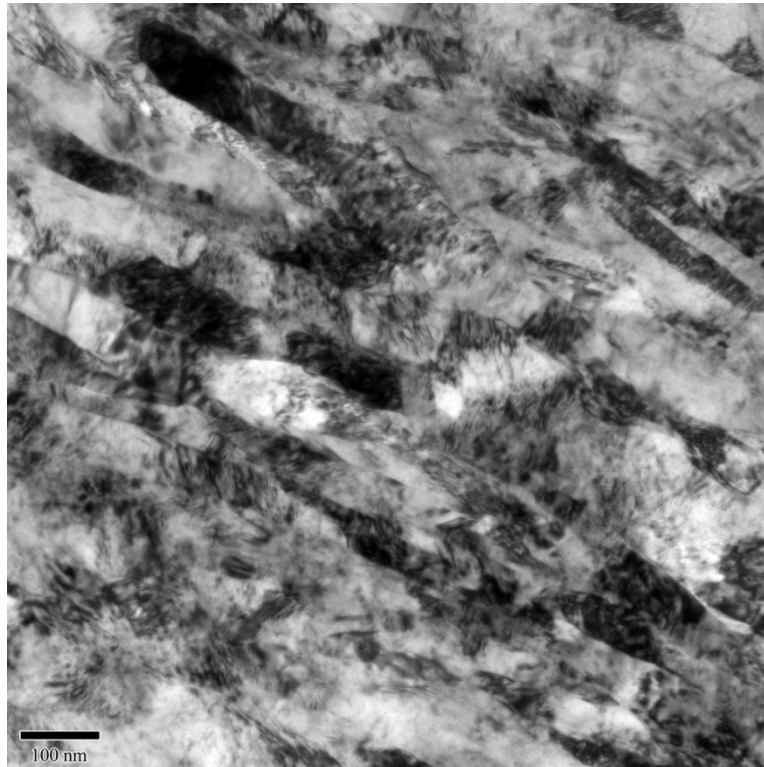


Figure 8 Bright field TEM image taken using the CM30 microscope showing the cold sprayed CuTa deposit prepared using the first batch of cryomilled powder. This region of the deposit is primarily copper. A highly deformed, sub-100 nm grain structure is visible throughout the deposit.

Figure 9 shows high resolution EDS analysis taken using the AC-STEM. These data show elemental maps of copper, oxygen, and tantalum in the copper rich region shown in Figure 7 and Figure 8. Importantly, no clusters of tantalum are found in this microstructure. In fact it is predominately copper with very little tantalum present as shown by the EDS spectrum, Figure 10.

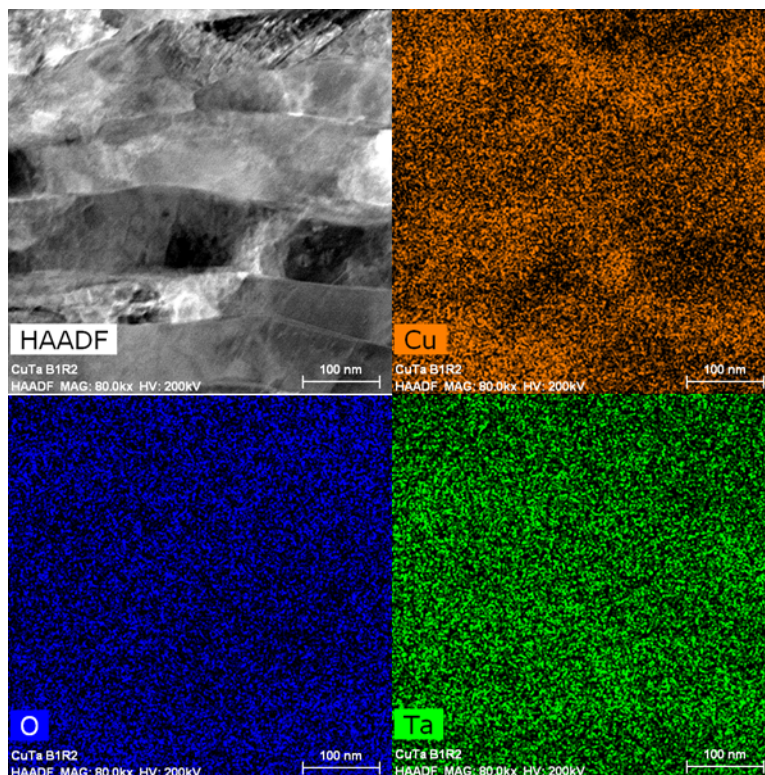


Figure 9 HAADF image and EDS patterns taken using the AC-STEM. The copper rich nanocrystalline structure in the deposit prepared using the first batch of cryomilled powder is shown. EDS maps reveal no detectable tantalum dispersion in the copper grain or along the copper grain boundaries. This suggests insufficient mechanically alloy of the copper and tantalum powders.

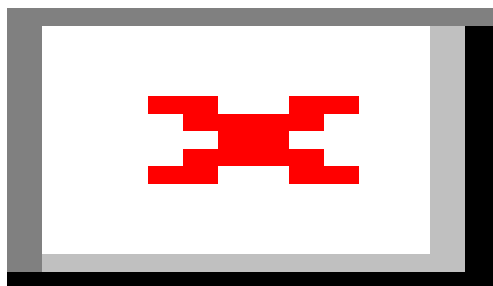


Figure 10 EDS spectrum from the region shown in Figure 9. The Tantalum peak, while real, is extremely small compared to the copper peak indicating that very little Ta is present in this region of the sample.

Figure 11 and Figure 12 show the microstructure of copper-tantalum deposit prepared using the second batch of cryomilled powder. This sample exhibits significant lack of mixing. Discrete regions of copper, tantalum, and copper oxide are clearly present. Importantly, regions of nanocrystalline copper are intermixed with large ribbons of tantalum, Figure 12, as confirmed by EDS mapping, Figure 13. Interestingly, high resolution imaging of the tantalum ribbon indicates that it contains grains that are on the order of 100 nm in size, Figure 14.

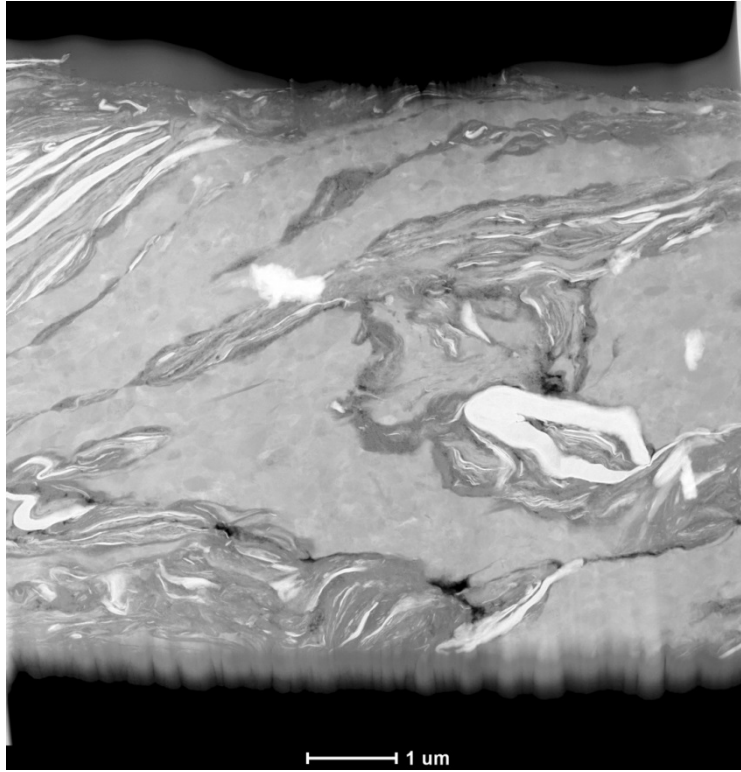


Figure 11 Z-contrast image taken using the AC-STEM showing the cold spray deposit prepared using the second batch of cryomilled powder. The white regions in the image are Ta, the gray regions are Cu, and the dark gray regions are copper oxide. Heterogeneous mixing is visible, consistent with the powder analysis.

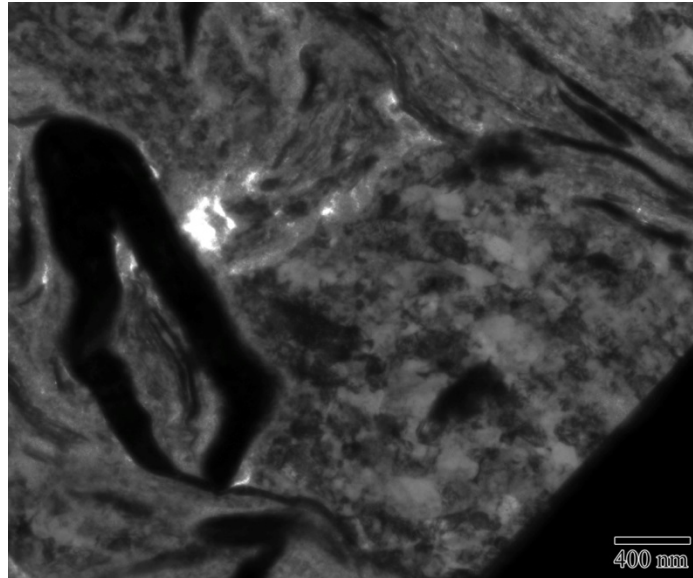


Figure 12. Bright field image taken using the CM30 microscope showing the CuTa deposit prepared using the second batch of CuTa powder. Regions of nanocrystalline copper are intermixed with large dark ribbons of tantalum.

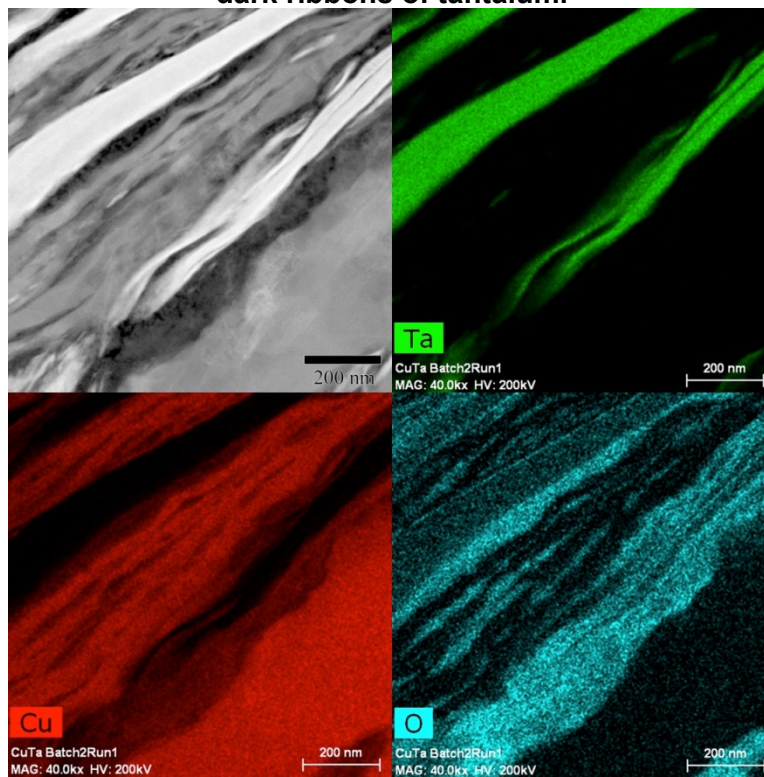


Figure 13 Upper left is HAADF image and EDS maps taken using the AC-STEM. This data from the cold spray deposit prepared using the second batch of cryomilled powder shows that copper, tantalum, and copper oxide are present as discrete regions in the deposit.

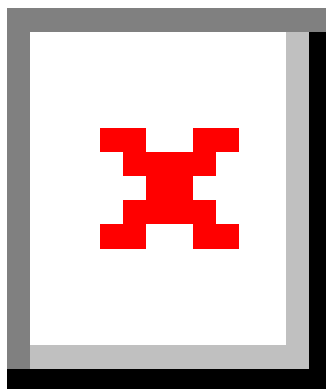


Figure 14 Bright field image taken using the AC-STEM, showing the microstructure within a tantalum ribbon. The tantalum exhibits considerable FIB damage making the grain structure difficult to resolve. Nevertheless, tantalum grains ~ 100nm in size are visible in the lower right of this image, confirming the presence of a nanocrystalline microstructure in the tantalum ribbon.

Microprobe analysis was used to quantitatively determine the copper-tantalum ratio in both deposits. The deposit made using the second batch of cryomilled powder contained considerably more oxide than the first batch. The presence of copper oxide impacted the desired 90at%Cu-10at%Ta ratio and may have contributed to lack of dispersion formation.

Table 1 Microprobe data showing CuTa deposit composition. Data from associated with the first batch of cryomilled powder is shown on the top row. Data associated with the second batch of cryomilled powder is shown on the second row. The deposit made using the second batch of cryomilled powder contained considerably more oxide than the first batch. This impacted the desired 90at%Cu-10at%Ta ratio and may have contributed to lack of dispersion formation.

Normalized Weight %				Atomic %			
Ta(Norm%)	Cu(Norm%)	O(Norm%)	Total(Norm%)	Ta(Atom)	Cu(Atom)	O(Atom)	Total(Atom)
12.73	83.73	3.54	100.00	4.56	81.69	13.75	100.00
13.71	77.89	8.27	100.00	4.19	67.39	28.34	100.00

CONCLUSIONS

Nanocrystalline copper-tantalum powders were prepared by cryomilling and were consolidated successfully using cold spray deposition. Consolidation using cold spray did preserve the nanocrystalline structure in the cryomilled powders. This experiment was motivated by recent reports that nanocrystalline copper-tantalum powders prepared by cryomilling are thermodynamically stable. Importantly, thermodynamically stable copper-tantalum powders, prepared elsewhere by cryomilling, contained a dispersion of tantalum atomic clusters in copper. This dispersion is thought to be critical to thermodynamic stability of nanocrystalline copper-tantalum. Microstructural analysis of copper-tantalum cryomilled powders and cold spray deposits shows that this dispersion was not achieved. However, despite the lack of a tantalum dispersion in copper, these initial experiments clearly demonstrate that solid-state consolidation of nanocrystalline copper-tantalum mixtures is possible without compromising the mixture's nanostructure using cold spray. This strongly suggests that a nanocrystalline copper-tantalum dispersion could be consolidated without compromising its nanostructure using cold spray.

REFERENCES

1. H. Gleiter, Nanostructured Materials: State of the Art and Perspectives, *NanoStructured Materials*, 1995, 6(1-4), p 3-14
2. C. C. Koch, Synthesis of nanostructured Materials By Mechanical Milling: Problems and Opportunities, *NanoStructured Materials*, 1997, 9(1), p 13-22
3. A. E. Romanov, Continuum Theory of Defects in Nanoscaled Materials, *NanoStructured Materials*, 1995, 6(1-4) p 125-134
4. Trelewicz, J. R. and C. A. Schuh (2007). "The Hall-Petch breakdown in nanocrystalline metals: A crossover to glass-like deformation." *Acta Materialia* 55: 5948-5958.
5. T. Frolov, K.A. Darling, L.J. Kecskes, Y. Mishin; Stabilization and strengthening of nanocrystalline copper by alloying with tantalum; *Acta Materialia* 60 (2012) 2158–2168
6. K.A. Darling, A.J. Roberts, Y. Mishin, S.N. Mathaudhu, L.J. Kecskes; Grain size stabilization of nanocrystalline copper at high temperatures by alloying with tantalum; *Journal of Alloys and Compounds* 573 (2013) 142–150
7. Julio Villafuerte; Considering Cold Spray for Additive Manufacturing; *Advanced Materials & Processes*, May 2014, pp. 50 – 52
8. R.E. Blose, B.H. Walker, R.M. Walker, S.H. Froes; New opportunities to use cold spray process for applying additive features to titanium alloys; *Metal Powder Report*, Volume 61, Issue 9, October 2006, Pages 30–37
9. J. Pattison, S. Celotto, R. Morgan, M. Bray, W. O'Neill; Cold gas dynamic manufacturing: A non-thermal approach to freeform fabrication; *International Journal of Machine Tools and Manufacture*, Volume 47, Issues 3–4, March 2007, Pages 627–634
10. H. J. Fecht, Nanostructure Formation By mechanical Attrition, *NanoStructured Materials*, 1995, 6(1-4), p 33-42
11. L. Ajdelsztajn, B. Jodoin, G. E. Kim, J. M. Schoenung, J. Mondoux, Cold Spray Deposition of nanocrystalline Aluminum Alloys, *Metallurgical and Materials --Transactions A*, 2005, 36A, p 657-666
12. P. Alkimov, V. F. Kosarev, A. N. Papyrin, A Method of Cold Gas-Dynamic Deposition, *Sov. Phys. Dokl*, 1990, 35(12), p 1047-1049
13. D. L. Gilmore, R. C. Dykhuizen, R. A. Neiser, T. J. Roemer, M. F. Smith, Particle Velocity and Deposition Efficiency in the Cold Spray Process, *Journal of Thermal Spray Technology*, 1999, 8(4), p 576-582
14. R. C. Dykhuizen, M. F. Smith, D. L. Gilmore, R. A. Neiser, X. Jiang, S. Sampath, Impact of High Velocity Cold Spray Particles, *Journal of Thermal Spray Technology*, 1999, 8(4), p 559-564
15. A. C. Hall, D. J. Cook, R. A. Neiser, T. J. Roemer, D. A. Hirschfeld, The Effect of a Simple Annealing Heat Treatment on the Mechanical Properties of Cold-Sprayed Aluminum, *Journal of Thermal Spray Technology*, 2006, 15(2), p 233-238
16. R. C. Dykhuizen and M. F. Smith, Gas Dynamic Principles of Cold Spray, *Journal of Thermal Spray Technology*, 1998, 7(2), p 205 - 212
17. A. C. Hall, L. N. Brewer, and T. J. Roemer, Preparation of Aluminum Coatings Containing Homogenous Nanocrystalline Microstructures Using the Cold Spray Process, *Journal of Thermal Spray Technology* Volume 17(3) September 2008, p 352-359
18. J. Eckert, Relationships Governing the Grain Size of Nanocrystalline Metals and Alloys, *NanoStructured Materials*, 1995, 6(1-4), p 431-416
19. Hamid Assadi, Frank Gärtner, Thorsten Stoltenhoff, Heinrich Kreye, "Bonding mechanism in cold gas spraying", *Acta Materialia* 51 (2003) 4379–4394
20. C. Borchers, F. Gärtner, T. Stoltenhoff, and H. Kreye, "Microstructural bonding features of cold sprayed face centered cubic metals", *Journal of Applied Physics*, Volume 96, Number 8, 2004, pp. 4288-4292

21. Qiang Wang, Dong Qiu, Yuming Xiong, Nick Birbilis, Ming-Xing Zhang, "High resolution microstructure characterization of the interface between cold sprayed Al coating and Mg alloy substrate", *Applied Surface Science* 289 (2014) 366– 369
22. Peter C. King, Christian Busch, Teresa Kittel-Sherri, Mahnaz Jahedi, Stefan Gulizia, 'Interface melding in cold spray titanium particle impact", *Surface & Coatings Technology* 239 (2014) 191–199
23. M. R. Rokni, C. A. Widener, and V. R. Champagne, "Microstructural Evolution of 6061 Aluminum Gas-Atomized Powder and High-Pressure Cold-Sprayed Deposition", *Journal of Thermal Spray Technology* Volume 23(3) February 2014, pp. 514-524P
24. M. Grujicic, J.R. Saylor, D.E. Beasley, W.S. DeRosset, D. Helfritch, "Computational analysis of the interfacial bonding between feed-powder particles and the substrate in the cold-gas dynamic-spray process", *Applied Surface Science* 219 (2003) 211–227
25. Tobias Schmidt, Frank Gärtner, Hamid Assadi 1, Heinrich Kreye, "Development of a generalized parameter window for cold spray deposition", *Acta Materialia* 54 (2006) 729–742
26. W. Y. Li, M. Yu, F. F. Wang, S. Yin, and H. L. Liao, "A Generalized Critical Velocity Window Based on Material Property for Cold Spraying by Eulerian Method", *Journal of Thermal Spray Technology*, Volume 23(3) February 2014, pp. 557-566
27. Chang-Jiu Li, Wen-Ya Li, Yu-Yue Wang, "Formation of metastable phases in cold-sprayed soft metallic deposit", *Surface & Coatings Technology* 198 (2005) 469– 473

DISTRIBUTION

1	MS1130	Aaron Hall	01832
1	MS1130	Pylin Sarobol	01832
1	MS1423	Blythe Clark	01111
1	MS0889	Nicholas Argibay	01851
1	MS0958	Christopher Diantonio	02734
1	MS0959	Deidre Hirschfeld	01832
1	MS0899	Technical Library	09536 (electronic copy)
1	MS0359	D. Chavez, LDRD Office	01911

